Astron. Astrophys. 319, 973–980 (1997)

ASTRONOMY
AND
ASTROPHYSICS

High velocity motions inside the HII region N 103 of the Large Magellanic Cloud⋆

P. Ambrocio-Cruz[1,2⋆⋆], **A. Laval**[1], **M. Marcelin**[1], **and P. Amram**[1]

[1] Observatoire de Marseille, 2 Place Le Verrier, F-13248 Marseille Cedex 04, France
[2] Instituto de Astronomía, UNAM, Apdo. 70-264, México, D.F., 04510, México

Received 6 June 1996 / Accepted 12 September 1996

Abstract. We have observed the HII region N 103 of the Large Magellanic Cloud with a scanning Fabry-Perot interferometer at Hα and [OIII]5007 wavelengths. The kinematics of this field shows high velocity motions. We discuss their origin: Supernova explosion or particularly strong stellar winds.

By calculating the energy input inside the gas, we show that it is unlikely that the high velocity motions are due to the stellar winds of the embbeded stars. Then the nebula N 103 is linked to two supernova remnants of different ages. The oldest one can be represented by a bubble, 152 pc wide, seen projected against the HII region, and probably lying at the edge of the HII region. The exciting stars of the nebula are actually members of the LMC cluster NGC 1850B; they provide a photon flux large enough to ionize the quiet part of the gas.

Key words: ISM: bubbles – ISM: HII regions – ISM: individual objects: N 103 – ISM: kinematics and dynamics – ISM: supernova remnants – galaxies: Magellanic Clouds

1. Introduction

Violent interrelations between the interstellar gas and the OB stars take place during short periods of the stellar lifetime. Their advent is mainly due to fast evolving stages of the stars, which are not well foreseen, i.e. strong stellar winds during the transitions to giant and supergiant phases, or disruption of the star when it is concluded by a supernova explosion. However such events let printed marks in the surrounding gas, even when their action has lasted but a short time; they produce shapes such as gaseous bubbles, archs and filaments. The features are non reversing as long as no other violent event happens; they can be detected much longer after they were formed, and have been studied in many galaxies.

However a complete overview of the occurence of the operative processes inside a galaxy requires the study of a large sample of these ionized features. The Large Magellanic Cloud (LMC) presents numerous advantages, which are well known (see i.e. Chu et al. 1994) for building up such an homogeneous sample of observations, and an Hα survey has been undertaken (Laval et al. 1987). Therefore not only the common properties of the ionized objects can come out, but also the kinematics and dynamics of different objects can be compared easily.

The nebula N 103 is the first HII region of this survey to be studied in the western part of the bar of the LMC. It is a peculiar object; many stars which are members of a rich cluster, NGC 1850, are apparently embedded in the nebula (Fig. 1). Such a situation is rare. Its neighbouring nebula, N 105, at a distance of only about 3'.5, does not appear so peculiar, and is ionized by an association of blue stars.

Moreover, on the NorthEastern edge of the nebula there is a small-diameter supernova remnant (SNR) mentioned by Mathewson & Clarke (1973) which is probably a member of the younger population of the cluster NGC 1850 (Chu & Kennicutt 1988). Studies at radio wavelengths (14.7 Ghz) performed by Milne et al. (1980) suggested that another SNR exists near NGC 1850 (Fig. 1). The association of an HII region and a SNR is frequent in the LMC (N 120, N 206, N 59, N 11, N 63....). The eventuality of a second SNR is an interesting clue to be studied.

In the following, we present the position and the environment of N 103 in the LMC (Sect. 2) and the observations and data reduction (Sect. 3). In Sect. 4, the results of the kinematics and flux determination are given. Section 5 is devoted to the comparison of the results with the usual models. Then a discussion of the different interpretations is given (Sect. 6), and the young NorthEastern SNR is presented (Sect. 7). Finally, general conclusions are examined.

Send offprint requests to: P. Ambrocio-Cruz

⋆ Based on observations collected at the European Southern Observatory

⋆⋆ Present address: Observatoire de Marseille, 2, Place Leverrier, 13248 Marseille Cedex 4, France

2. Main characteristics and local environment of N 103

N 103 is a nebula of 9' x 12' angular dimensions (Fig. 1) which corresponds to 131 x 175 pc for a distance of 50 kpc (Feast 1991 and Panagia et al. 1991) to the LMC. This bubble-like nebula has a strong ionization front to the East, well separated from another nebula DEM85, and a long filament in the western part. N 103 is situated in the very western side of the bar of the LMC, in a region rich with star clusters, such as NGC 1850.

NGC 1850 is a young double cluster (Robertson 1974; Fischer et al. 1993; Vallenari et al. 1994; Gilmozzi et al. 1994) with a center-to-center separation of 30 arc sec and it is located near the eastern ionization front of N 103. The age of the oldest cluster (NGC 1850A) has been determined by several authors. Fischer et al. (1993) found an age of 90 $\pm$ 30 Myr, Vallenari et al. (1994) estimated 50-70 Myr while Gilmozzi et al. (1994) found 50$\pm$10 Myr. For the youngest cluster (NGC 1850B), they have determinated an age of 6 $\pm$ 5 Myr (Fischer et al. 1993), 8-10 Myr (Vallenary et al. 1994) and 4.3 $\pm$ 0.9 Myr (Gilmozzi et al. 1994).

Gilmozzi et al. (1994) from observations with the Hubble Space Telescope, have studied the stellar content of NGC 1850. They have estimated that the total number of member stars brighter that B=22.1 is 4 times higher for NGC 1850A than for NGC 1850B (respectively 3530 and 870). They have identified in the young cluster 64 stars between 7-40 $M_\odot$ and have determined a slope of the initial mass function (IMF) f(m) α $m^{-2.6}$. But only about 30 stars of this cluster have an effective temperature above 20000 ^{o}K and among them, about half have a luminosity higher than 3 x $10^4 L_\odot$. They have estimated that a total Lyman-continuum photon flux of $\sim 4 \times 10^{49}$ photons s^{-1} is emitted by NGC 1850B. From the color-magnitude diagram of the old cluster, they have determined that the most massive unevolved stars of the old cluster have a mass of 6 $M_\odot$.

Fischer et al. (1993) have studied the dynamics of this young binary cluster. They have determined that the stars of the older cluster, which have an initial mass greater than 8 $M_\odot$, are ejected from the cluster. Thus no star of the older cluster can be massive enough to ionize the gas. They have calculated a mean cluster velocity v = 251.4$\pm$2.0 km s^{-1}. Rohlfs et al. (1984) from 21 cm observations found two components of HI gas with velocities 260 km s^{-1} and 291 km s^{-1}.

Israel et al. (1993) have detected a ^{12}CO cloud in the direction of DEM85 (East of N 103). They could not measure its systemic velocity; which probably means that this cloud is small and/or faint.

3. Observations and data reductions

An Hα and [OIII]5007 survey of the Magellanic Clouds is being carried out at the European Southern Observatory of la Silla, (Le Coarer et al. 1993 for the SMC and Laval et al. 1987 for the LMC). A detailed description of the equipment used for the observations and reduction explanations can be found in Le Coarer et al. (1992 and 1993) and Georgelin et al. (1994). We recall here some general aspects of the instrument and reduction. The instrument is a 36 cm diameter telescope equipped with a focal reducer, a scanning Fabry-Perot interferometer, a photon counting camera and a series of interference filters.

We obtain images with a field of view of $38' \times 38'$ (covered by the 256 x 256 pixels of the photon counting camera) and an angular resolution of 9" $\times$ 9".

We have used the Fabry-Perot interferometer with interference order p = 796 at the Hα line, offering a free spectral range of 377 km s^{-1} and a spectral sampling of 16 km s^{-1} with 24 scanning steps. When used at the 5007 line, the interference order is p=1041, offering a free spectral range of 288 km s^{-1} and a sampling of 7 km s^{-1} with 40 scanning steps, allowed by the narrow FWHM of the [OIII] gaussian profiles, and calibrated by a Helium lamp. The filters used for the LMC are H$\alpha_{(LMC)}$ λ = 6569 Å, $\delta\lambda$ = 16 Å and [OIII]$_{(LMC)}$ λ = 5015 Å, $\delta\lambda$ = 17 Å.

To obtain spatial information of the velocities, we separate the local components by Gaussian profile fitting. Calibrating the fluxes may be done only indirectly, generally with HII regions for which absolute photometry exists. For N 103 we have used the flux measured by Caplan & Deharveng (1985) of the HII region DEM 85 situated 2' East of N 103.

4. Physical data of the nebulae in the field

4.1. The HII region DEM 85

DEM 85 is a typical bright circular HII region of 90" angular diameter (22 pc for a distance of 50 kpc of the LMC), situated 2' East of N 103 (Fig. 1), its Hα emission seems to come from a homogeneous and regular sphere. DEM 85 does not show any expansion motion; a single Gaussian profile with FWHM = 22 km s^{-1} is displayed in its Hα kinematic field, centered at the heliocentric radial velocity 260 km s^{-1}. The FWHM is systematically corrected from the instrumental function; the mean signal/noise ratio is S/N = 66.

The main characteristics of DEM 85 are given in Table 1. We have corrected the surface brightness value measured photoelectrically by Caplan & Deharveng (1985), adopting an average colour excess of $E_{(B-V)}$ = 0.18 mag (Gilmozzi et al. 1994). The emission measure and the rms electron density have been calculated in the same way as for the N 120 complex (Laval et al. 1992).

4.2. The nebula N 103

Fig. 1 shows our Hα and [OIII] images (obtained by integrating our kinematic frames pixel per pixel) of the nebula N 103, which (at faint levels of the Hα emission) has an elliptical shape. In the Hα line N 103 looks like a shell, the emission of which is well limited and enhanced to the East, along an ionization front, which separates it from DEM 85. The Hα emission decreases towards the West.

The average heliocentric velocity for the total Hα emission is 252 km s^{-1} with a FWHM=53 km s^{-1}. It gives the systemic velocity of the ionized gas. The high value of FWHM suggests the existence of several velocity components.

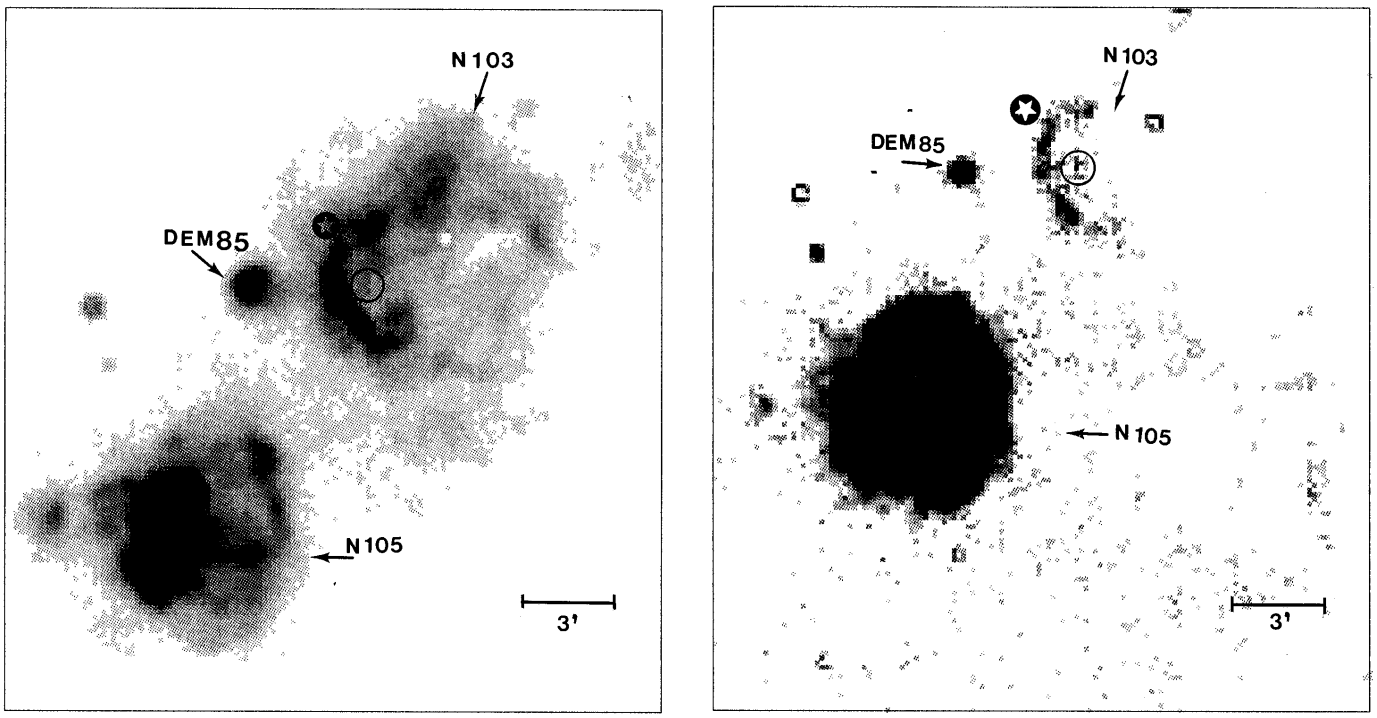

Fig. 1. Hα (on the left) and [OIII] (on the right) images of the nebulae N 103, N 105 and DEM85. The positions of the small SNR and the stellar cluster NGC 1850 are show by an asterisk and a circle respectively. North is at the top and east is to the left

Fig. 2 shows several examples of the Hα emission as detected in the CIGALE monochromatic maps corresponding to three wavelength maps centered at the velocities 282 km s^{-1}, 250 km s^{-1} and 235 km s^{-1}. While the map corresponding to 282 km s^{-1} displays the features corresponding to the outer share without detection to the South West, the map corresponding to 235 km s^{-1} is very bright in the inner share and also displays filamentary features to the South West. The two images present filamentary features to the North.

Fig. 3 shows some examples of the Hα profile shape and of their location across the nebula. Note that the kinematic field displays an envelope of Gaussian profiles sourrounding a zone of complex Hα line profiles. The complexity of profiles increases in the direction of the cluster NGC 1850. We have fitted Gaussians with FWHM=32 km s^{-1} to the observed profiles. We find a main component at an average velocity of 252 $\pm$ 3 km s^{-1} which covers the total field of observation. This component has a highly variable intensity ($2 < S/N < 122$) (Fig. 2). Then a redshifted velocity component is centered between 275 km s^{-1} and 280 km s^{-1} with $2 < S/N < 40$. The most extreme redshifted velocity value is 313 km s^{-1} (S/N = 13) and is located near NGC 1850. Finally, we detect a blueshifted velocity component centered between 220 and 225 km s^{-1} with $2 < S/N < 40$. The most extreme blueshifted velocity value is 200 km s^{-1} (S/N = 12) and is also located near the cluster NGC 1850.

Hereafter we name "HII region" the main component with the velocity of 252 km s^{-1}. In Table 1, we have quoted the radius (R) of the region DEM 85 and N 103, obtained from our Hα frames, the Hα surface brightness (S(Hα)) of the HII region, taking as flux calibrator the flux of the HII region DEM 85 measured photoelectrically by Caplan & Deharveng (1985). We correct the surface brightness value for interstellar extinction and we calculate the emission measure (EM) and the rms electron density (n_e) in the same way as explained in Sect. 4.1. The rms electron density of the HII region has been evaluated by assuming an homogeneous sphere of radius R. We have also quoted the heliocentric velocity (V_s) of the HII region.

In the [OIII]5007 line, a strong emission is detected for the nebula N 105, while for N 103 only the cluster NGC 1850 and a weak arch-like filament near this cluster are visible (Fig. 1). The geometrical center of this filament coincides with the geometrical center of the Hα emission. The geometrical radius of [OIII] emission is 27 pc. The systemic velocity for the total [OIII] emission is 263 km s^{-1}, with a broad gaussian profile of FWHM=63 km s^{-1}. At high spatial resolution, the profiles are complex. Fig. 4 shows an example of the [OIII] profile shape. We have fitted gaussians with FWHM = 7 km s^{-1} to these profiles. We find a blueshifted velocity component, with a lower limit of 240 km s^{-1} (S/N$\sim$ 3) and a redshifted velocity component with an upper limit of 281 km s^{-1} (S/N$\sim$ 4). The morphology of these components does not agree with the morphology of the two high velocity components of Hα emission.

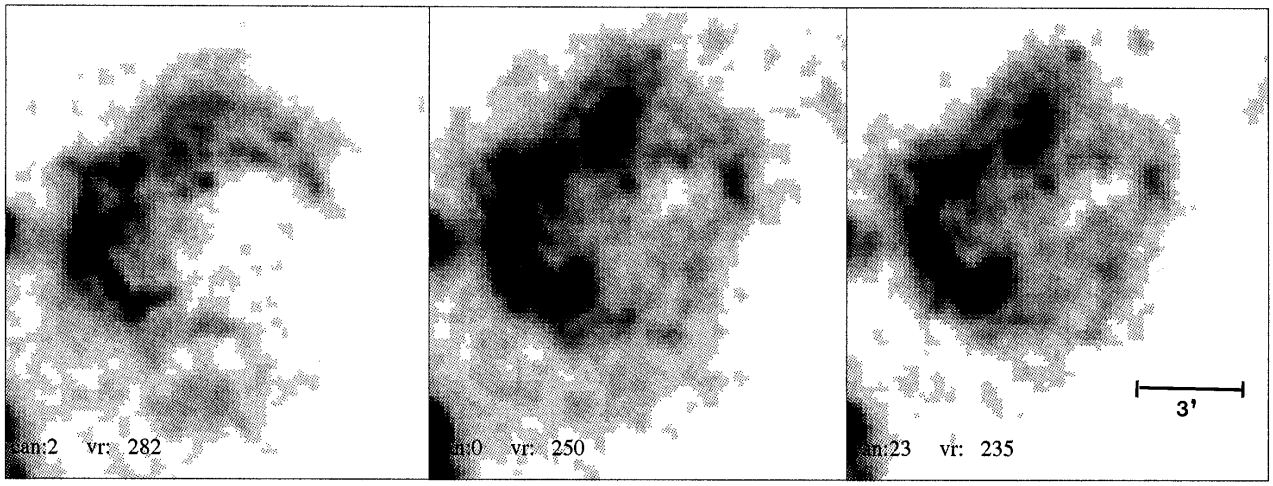

Fig. 2. Wavelength Hα maps of N 103 corresponding to the following heliocentric radial velocity range: 282 ± 8 km s^{-1}, 250 ± 8 km s^{-1}, 235 ± 8 km s^{-1}

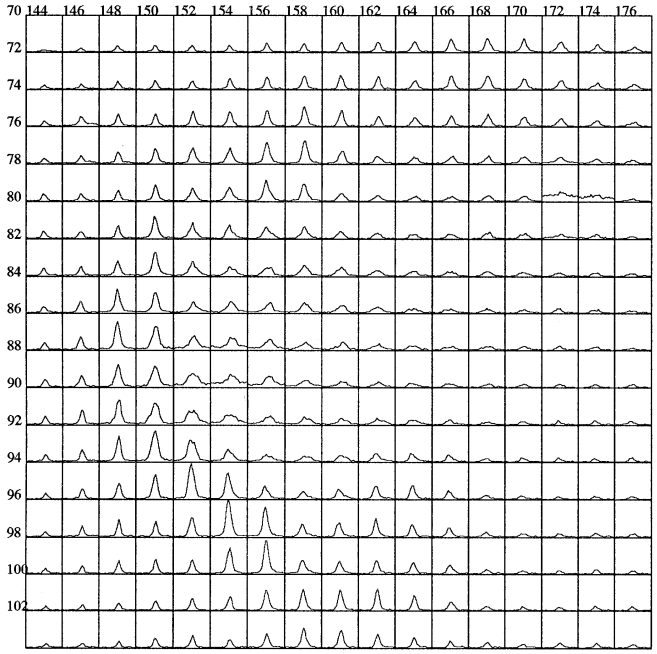

Fig. 3. Radial velocity profiles of the central part of the nebula N 103. Hα profiles are shown inside squares of 18" $\times$ 18". Complex line profiles can be seen inside the bubble.

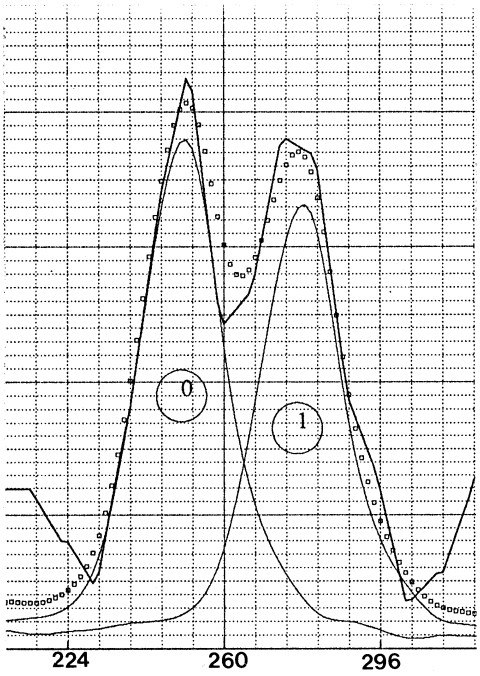

Fig. 4. Example of the [OIII] radial velocity profiles of N 103. This profile is obtained over an area of 18" $\times$ 36". The x-coordinate gives the radial velocity in km s^{-1} and y-coordinate gives the intensity of the line in arbitrary units.

5. Interpretation of the observations

5.1. The bubble

As shown in Sect. 4, by means of the Hα Fabry-Perot observations, we distinguish three velocity components: an intense component corresponding to the HII region and two fainter components. Both faint components reveal a bubble 152 pc in diameter, this value being measured from the more extended component (the redshifted one).

The broadening and splitting of the line profiles increase near the position of the cluster, this splitting can be explained by an expansion of the bubble (57 km s^{-1}), deduced from the extreme velocity values.

The Hα surface brightness and rms electron density of this bubble are given in Table 1. The main difficulty for N 103 is to discriminate the part of gas coming from the HII region, and the one belonging to the high velocity layers. Both are seen along the line of sight towards N 103: the line profiles show everywhere

Table 1. Main Hα characteristics of the nebulae

	HII Region DEM 85	HII Region N 103	Bubble
R	11	82	76
S	11.7	3	2.45
EM	1338	346	280
n_e	7.8	2	5
V_s	260	252	252
V_e	-	-	57

NOTES:
R : Linear radius (pc)
S : Surface brightness (x10^{-5} erg cm^{-2} s^{-1} sr^{-1})
EM : Emission measure (cm^{-6} pc)
n_e : rms electron density (cm^{-3})
V_s, V_e : Heliocentric systemic velocity and expansion velocity (km s^{-1})

the presence of the quiet component. Thus the uncertainty of the flux of the high velocity layers, given by the Gaussian fitting , is about 50%. The rms electron density has been evaluated by assuming a shell thickness $\Delta R \sim R/12$. The uncertainty of the evaluated flux leads to an indetermination of 21% on the electron density and 60% on kinetic energy. The uncertainty on the radius (21%) leads to an additional uncertainty on electron density of 21% and the uncertainty on the expansion velocity leads to an additional uncertainty of 18% on the kinetic energy. Therefore the mass concentrated in this shell is evaluated to be between 9×10^3 and $3 \times 10^5 M_\odot$, calculated in the same way as for the N 120 complex (Laval et al. 1992), and leads to a kinetic energy of $3 \times 10^{50} - 9 \times 10^{51}$ ergs.

5.2. The models

In order to explain the motions inside N 103, we have applied Supernova Remnant and Stellar Wind models. According to the model of Chevalier (1974) for a SNR in the radiative phase, a supernova driven bubble, of radius R (in pc) and expansion velocity V (in km s^{-1}), requires an energy E (in units of 10^{50} ergs):

$$E = 5.3\text{x}10^{-7} n_o^{1.12} V^{1.4} R^{3.12}$$

where n_o is the ambient density.

The age t (in units of 10^4 years) is obtained from the relation $t = 30.4 \frac{R}{V}$ (Chevalier 1974).

According to the model of a supersonic stellar wind driven bubble of Weaver et al. (1977), this bubble of radius R (in pc) and expansion velocity V (in km s^{-1}) requires a wind power L (in units of 10^{36} erg s^{-1}), which is given by:

$$L = 3.35 \times 10^{-7} R^2 n_o V^3$$

where n_o is the ambient density.

The age t (in units of 10^6 years) of the bubble is obtained from the relation $t_6 = 0.59 \frac{R}{V}$ (Weaver et al. 1977).

Table 2. Hα parameters derived from the models

	Bubble driven by SNR	Bubble driven by stellar wind
n_o(cm^{-3})	0.2-6	0.2-6
E or L	$2 \times 10^{51} - 8 \times 10^{52}$erg	$7 \times 10^{37} - 2 \times 10^{39}$erg s^{-1}
t ($\times 10^5$ years)	4	8

NOTES:
n_o : Ambient density
E, L : Required energy
t : Age

The pre-shock density, n_o, of a medium traversed by a radiative shock can be estimated from the shock radiated Hα surface brightness, $S_{(H\alpha)}$ in erg cm^{-2} s^{-1} sr^{-1} and the shock velocity, V_e, according to the following relation (Cantó & Rodríguez, 1986):

$$n_o = \frac{S_{(H\alpha)}}{6.64 \times 10^{-10} V_e^2}$$

valid for $V_e < 150$ km s^{-1} and a spherical shock wave. When $S_{(H\alpha)}$ is the surface brightness of both hemispheres of the shell (the red and blue component), the second member of the equation must be divided by 2. We then obtain $n_o \simeq 6$ cm^{-3}. When the SNR is large, and therefore old, an isothermal assumption may represent better the situation and the pre-shock density is given by: $n_o = \left(\frac{C}{V}\right)^2 n_e$. It gives $n_o = 0.2$ cm^{-3}.

Table 2 lists all the parameters derived from these two models, using the observed values of Table 1.

6. The origin of the bubble N 103

Does one of the two possible models match at best the Hα observations?

6.1. The stellar winds

The monochromatic images of the field (Fig.1) show the presence of several emitting objects. In the Hα line three nebulae are conspicuous : N 103 (DEM 84), N 105 (DEM 86), and DEM 85. In the [OIII]5007 line only two nebulae are bright; N 103 is very faint. Such an image is not expected for nebulae surrounding stars with strong stellar winds. It demonstrates the lack of stars able to ionize the oxygen atoms in O^{++}, then hotter than 37000K, and thus more massive than 25 solar masses (spectral type O7). Taking for the parameters of the stellar winds for such stars : a terminal velocity of 2000km s^{-1}, and a mass loss of 10^{-6} $M_\odot$ year^{-1} (Walborn et al 1995), the wind power for one star is found to be 10^{36} erg s^{-1}.

When one compares this value to Table 2, the energetic input in N 103 would thus require the presence of at least 70 O7 stars in the cluster NGC 1850B (and none more massive star), when

we try to explain the bubble only by the action of stellar winds. Such a number of O7 stars is not known in the cluster. Though not so efficient, the winds of O8III-V to B0I stars cannot be negligible. Taking a classic mass function determined for the LMC (Massey et al. 1995), with the wind velocity from Walborn et al. (1995) and a mass loss rate of 0.5×10^{-6} $M_\odot$ year^{-1} for the 15-25 solar mass bin of stars, and 10^{-7} $M_\odot$ year^{-1} for the 7-15 solar mass bin, the total contribution is computed to be equivalent to the gas energy of N 103 when we have:

41 stars of 25 solar masses (type O7)

68 stars in the range 15-25 solar masses

240 stars in the range 7-15 solar masses (only B1-B2 I stars).

In this last bin, the latest spectral type possible is B2 because the wind parameters decrease dramatically for later types, and thus their winds do not transfer much energy to the ambient medium.

Such a large number of O stars does not seem to exist in NGC 1850, because by taking the initial mass function determined by Gilmozzi et al. (1994) for the younger cluster we find that only 17 stars are in the mass bin of 15-25 $M_\odot$ and 7 in 25-40 $M_\odot$. We must also keep in mind some discrepancies found by Oey & Massey (1995), on the consistancy of the models of stellar wind driven bubble. However, the lack of massive stars is so large in N 103 that it cannot be compensated by a model improvement only.

6.2. An explosion of Supernova

The assumption of energy input by a supernova (SN) explosion is plausible since the typical value of such an event falls inside the range of energy observed in N 103 (Table 2).

The higher value that we have found for the energy, seems unrealistic for a bubble of such a size. It seems to indicate either that the evolution phase does not allow the application of the relation by Cantó and Rodríguez, or that the initial conditions before the SN explosion, were changed.

The initial conditions are actually different when active stellar winds have made cavities around the more massive stars. Then the expansion of the SNR has occurred for a certain time inside a cavity, and other models examine such cases (McCray & Kafatos 1987).

The lower value of the energy that we have found is in agreement with the value of energy input by an explosion of supernova. ROSAT observations of the LMC done by Snowden & Petre (1994) show effectively an extended X-ray emission of N 103, centered close to the position of the cluster.

Moreover, Oey (1996a,b) has demonstrated that the present-day stellar content can be used to predict the number of previous supernovae. We have considered the IMF derived by Gilmozzi et al. (1994) for NGC 1850B, and following Oey, we have estimated the number of "missing" massive stars to be of 3 stars of 40-60 $M_\odot$, 1 star of 60-85 $M_\odot$ and perhaps 1 star of 85-120 $M_\odot$. Therefore, the most plausible explanation is that we observe gas motions due to a SN explosion inside a cavity made by previous stellar winds and one or several SN explosion(s). From the ages of the stellar cluster and of the cavity, the latest explosion should have occured about 4.10^6 years ago. From stellar models by Schaerer et al. (1993) stars of 40 $M_\odot$ have a lifetime of the order of 5.10^6 years.

Table 3. Parameters derived from the models for the small [OIII] shell.

	SN driven model	Stellar Wind driven model
E or L	$2 \times 10^{49} - 8 \times 10^{50}$erg	$4 \times 10^{35} - 1 \times 10^{37}$erg s^{-1}
t ($\times 10^5$ years)	4	8

NOTES:
E, L : Required energy
t : Age

6.3. The HII region

It is the more intense component in the field, as faint as S/N=2 to the West, and as bright as S/N=122 to the East. The splitting of the [OIII] line profiles (Fig. 4) can be explained by an expansion of the gas of 21 km s^{-1}, deduced from the velocity components (Sect. 4.2). In order to explain this expansion we have applied both models, SNR and Stellar Wind. For the value of the pre-shock density we used the two values listed in Table 2, because the expansion centers of both shells, Hα and [OIII], are very near each other (Sect. 4.2), showing that the previous ambient medium was the same. Table 3 lists the parameters derived using the values of radius quoted in Sect. 4.2.

The expansion of the [OIII] emission can be explained by the stellar wind of one (or at most 10) O7 star(s) of the youngest stellar cluster actuating over interstellar medium. There should be only a few O7 stars, as shown from the faint [OIII] emission. Greve et al. (1990) observed photometrically the 3 brightest stars situated between 20" and 1' far from the center of the young cluster. The colors and absolute magnitudes show that they are early B supergiants. Therefore the O stars should be nearer to the center of the cluster.

The enhancement of Hα and [OIII] emission in the Eastern region of N 103 may be due to a gradient in density. Such a density gradient is probably the consequence of the existence of a ^{12}CO cloud in the direction of DEM85 (Israel et al. 1993).

We have also determined the number of ionizing photons by considering the radio continuum and Hα luminosity of the HII region.

For the radio continuum, we have used the data of the Parkes 6-cm survey of McGee et al. (1972) because 6-cm observations are less perturbed by the presence of non-thermal sources than the Molonglo 73-cm observations (Clarke et al. 1976). For the source MC22 (N 103 and DEM85) of the 6-cm survey we have calculated a flux of ionizing photons 1.2×10^{50} phot s^{-1}. For the same area as MC22 but considering the Hα luminosity measured in our survey, we find 1.4×10^{50} phot s^{-1}. It is larger than the number determined by radio continuum, because the total

Hα luminosity includes the emission of the high-velocity layers. When we subtract the emission corresponding to the N 103 bubble, we find a number of ionizing photons 8.4×10^{49} phot s^{-1}. Then the flux of ionizing photons derived from the 6-cm data is larger than the flux derived from the Hα image. The radio continuum provides a more accurate measure of the ionizing photons because it is free of extinction.

In order to quantify the interstellar reddening in the region of N 103 and DEM85 we have compared the free-free emission and the Balmer emission. Using the derivation presented by Caplan & Deharveng (1986) for the theoretical relation between the observed Hα flux and the radio continuum emission at some frequency ν, we have determined the extinction at Hα, and assuming $A_v = 1.31 A_{H\alpha}$ we determine an average colour excess of $E_{B-V} = 0.16$ mag. It is in good agreement with the value calculated by Gilmozzi et al. (1994) of $E_{B-V} = 0.18$ mag for the cluster NGC 1850. Then it is justified to take the same color excess for DEM85 as for N 103 (Sect. 4.1).

In order to compare the UV flux of the present stars to the number of ionizing photons of the HII region N 103 only, we have considered its Hα luminosity (the emission corresponding to the bubble N 103 has been subtracted). We find 7×10^{49} ionizing phot s^{-1}. This is larger than the flux emitted by NGC 1850B by a factor ≤ 2. It probably comes from an overestimation of the Hα flux attributed to the velocity component at 250 km s^{-1}. It could be due as well to the existence of other exciting stars, but none other blue stars are known in the field.

Then the cluster NGC 1850B is actually the ionizing source for the Hα and [OIII] emission of the 250 km s^{-1} component. Moreover the velocity of this HII region agrees with the mean velocity of NGC 1850 calculated by Fischer et al. (1993) (Sect. 2).

7. The young SNR N 103B

The SNR N 103B , situated to the North-Eastern edge of the nebula, has been intensively studied spectroscopically once it has been identified by radio means (Danzinger & Dennefeld 1976; Dopita 1979; Danzinger & Leibowitz 1985; Chu & Kennicutt 1988). Previous studies have shown that it is related to the nebula N 103, and that the dense knots are at high temperature. It is also noted that surprisingly the [OIII] 5007 line is weaker than the Hβ line, unlike high-temperature regions in other SNRs of the LMC ; [NII]6584 is neither particularly strong.

We have observed this SNR with the CIGALE instrument attached to the ESO 1.5m telescope, in order to get a better spatial resolution (2.5" per pixel); the free spectral range was the same as previously, 376km s^{-1}, with a spectral resolution slightly lower : 18.8 km s^{-1}. The two highly luminous knots, of high density, as shown by Danzinger & Leibowitz from the [SII] lines, have dimensions as small as 4"x5", and are surrounded by a more extended low density region of 17.5"x27.5", which is 4x7 pc at a distance of 50 kpc. Then the SNR is very probably young, though its velocity range is not so high as in other SNRs of comparable size such as N 132D. One wide velocity component is found. The lower limit of the FWHM of the fitted Gaussian, once the contributing emission from the underlying HII region is subtracted, is 241 km s^{-1}, much larger than the 140 km s^{-1} found by Dopita (1979) from the [OII]3726 lines, and better in agreement with the extent of the faint emission visible in the spectrum taken by Chu & Kennicutt (1988).

8. Conclusions

The radial velocity field of N 103 shows the existence of high velocity motions inside this nebula. They can be interpreted as showing the expansion of a bubble 152 pc in diameter with an expansion velocity of 57 km s^{-1}.

In order to explain these motions, we have applied Supernova Remnants (radiative phase) and stellar wind models. The energy value that we have calculated, the lack of a large number of O stars with a strong stellar wind, and the X-ray emission suggest that these high velocity motions are issued from an old SN explosion. The number of already disappeared massive stars in the younger cluster, may be as high as 5. Then, the nebula N 103 presents the rare opportunity of being linked to 2 SNRs. It is presumably related to the higher probabiblity of finding evolved stars in the LMC clusters than in OB associations. A SN explosion yields the ejection of metal rich gas together with the formation of a shock front. The presence of several remnants in the region could suggest that SN explosions have triggered the second episode of star formation, when a sufficient quantity of gas was still remaining. However the age of the youngest population of NGC 1850 is larger than the age of the observed SNRs. Have previous explosions of SN efficiently triggered the formation of the youngest cluster?

The precursors of the supernovae are likely associated with the younger cluster NGC 1850B, since the most massive unevolved stars of the older cluster have a mass of 6 $M_\odot$ (Gilmozzi et al. 1994). The latest SN explosion should have occurred 4.10^6 years ago. It is strange that the [OIII] emission of the bubble N 103 is not visible. But it has been noted that the young SNR also presents a weaker [OIII] emission than expected from its metallic abundance compared to other SNRs of the LMC (Sect. 7).

The order of succession of the nebulae along the line of sight is not obvious. The HII region extends all over the observed field, but it presents the same decrease in intensity towards the West as the bubble. It shows that the western direction undergoes the minor density pressure. On the other hand, the bubble is limited towards the East by the ionization front. Moreover the systemic velocities of the bubble and the HII region are the same. All these facts suggest that the remnant is physically related to the HII region surrounding the cluster. Therefore either the bubble and the HII region are neighbours seen along the same line of sight, or the bubble occurs at the edge of the HII region, and lets subsist a thick outer layer of non shocked gas.

The heterogeneity of the interstellar medium reflects such a chaotic history. The uncertainty on the value of the pre-shock density may occur because the stellar wind of the more massive stars of the youngest stellar cluster is actuating over the inter-

stellar medium before the supernova explosion. On the other hand, the bright ionization front in the eastern region of N 103 may be due to a density gradient towards the molecular cloud.

The Hα heliocentric systemic velocity of the N 103 nebula shows that it is related to the 260km s^{-1} HI layer of the LMC.

Acknowledgements. P. Ambrocio-Cruz wishes to thank the support of the Ville de Marseille and DGAPA-UNAM (grants IN 102192) during the realization of this work. Also she thanks Dr. M. Rosado for valuables comments and discussions. We are grateful to Didier Cahalo for his collaboration.

References

Cantó J., Rodríguez L.F., 1986, Rev. Mex. Astron. Astrofis. 13, 57
Caplan J., Deharveng L., 1985, A&AS 62, 63
Chevalier, R. A., 1974, ApJ. 188, 501
Chu Y-H., Kennicutt R.C., 1988, AJ 96, 1874
Chu Y-H., Wakker B., Mac Low M.M., Garcia Segura G., 1994, AJ 108, 1696
Danzinger I.J., Dennefeld M., 1976, PASP 88, 44
Danzinger I.J., Leibowitz E.M., 1985, MNRAS 216, 365
Dopita M.A., 1979, ApJS 40, 455
Feast M.W., 1991, In the Magellanic Clouds, IAU Symposium, No. 148, p.1
Fischer P., Welch D.L., Mateo M., 1993, AJ 105, 938
Georgelin Y.M., Amram P., Georgelin Y.P. et al., 1994, A&AS 108, 513
Gilmozzi R., Kinney E.K., Ewald S.P. et al., 1994, ApJ 435, L43
Greve A., Van Genderen A.M., Laval A., 1990, A&AS 85, 895
Israel F.P., Johansson L.E.B., Lequeux J., et al., 1993, A&A 276, 25
Laval A., Boulesteix J., Georgelin Y.P., et al., 1987, A&A 175, 199
Laval A., Rosado M., Boulesteix J. et al., 1992, A&A 253, 213
Le Coarer E., Amram P., Boulesteix J. et al., 1992, A&A 257, 389
Le Coarer E., Rosado M., Georgelin Y.P., et al., 1993, A&A 280, 365
Massey P., Lang C.C., Degioia-Eastwood K., Garmany C.D., 1995, ApJ 438, 188
McCray R., Kafatos M., 1987, ApJ 317, 190
McGee, R.X., Brooks, J.W., Batchelor, R.A., 1972, Aust. J. Phys. 25, 581
Mathewson D.S., Clark D.H., 1973, ApJ 180, 725
Milne D.K., Caswell J.L., Haynes R.F., 1980, MNRAS 191, 469
Oey M.S., Massey P., 1995, ApJ 452, 210
Oey M.S., 1996a, ApJ 465, 231
Oey M.S., 1996b, ApJ, in press
Panagia, N., 1973, AJ 78, 929
Panagia N., Gilmozzi R., Adorf H-M. et al., 1991, ApJ 380, L23
Robertson J.W., 1974, A&AS 15, 261
Rohlfs K., Kreitschmann J., Siegman B.C., Feitzinger J.V., 1984, A&A 137, 343
Schaerer D., Meynet G., Maeder A., Schaller G., 1993, A&AS 98, 523
Snowden S.L., Petre R., 1994, ApJ 436, L123
Tuohy I.R., Dopita M.A., Mathewson D.S., 1982, ApJ 261, 473
Vallenari A., Aparicio A., Fagotto F. et al., 1994, A&A 284, 447
Walborn N.R., Lennon D.J., Haser S.M. et al., 1995, PASP 107, 104
Weaver R., Mc Cray R., Castor J. et al., 1977, ApJ 218, 377

This article was processed by the author using Springer-Verlag LaTeX A&A style file *L-AA* version 3.